

# Cobalt Dopant with Deep Redox Potential for Organometal Halide Hybrid Solar Cells

Teck Ming Koh,<sup>[a, b]</sup> Sabba Dharani,<sup>[a, b]</sup> Hairong Li,<sup>[a]</sup> Rajiv Ramanujam Prabhakar,<sup>[a]</sup> Nripan Mathews,<sup>\*,[a, b, c]</sup> Andrew C. Grimsdale,<sup>\*,[b]</sup> and Subodh G. Mhaisalkar<sup>[a, b]</sup>

In this work, we report a new cobalt(III) complex, tris[2-(1*H*-pyrazol-1-yl)pyrimidine]cobalt(III) tris[bis(trifluoromethylsulfonyl)imide] (MY11), with deep redox potential (1.27 V vs NHE) as dopant for 2,2',7,7'-tetrakis-(*N,N*-di-*p*-methoxyphenylamine)-9,9'-spirobifluorene (spiro-OMeTAD). This dopant possesses, to the best of our knowledge, the deepest redox potential among all cobalt-based dopants used in solar cell applications, allowing it to dope a wide range of hole-conductors. We demonstrate the tuning of redox potential of the Co dopant by in-

corporating pyrimidine moiety in the ligand. We characterize the optical and electrochemical properties of the newly synthesized dopant and show impressive spiro-to-spiro<sup>+</sup> conversion. Lastly, we fabricate high efficiency perovskite-based solar cells using MY11 as dopant for molecular hole-conductor, spiro-OMeTAD, to reveal the impact of this dopant in photovoltaic performance. An overall power conversion efficiency of 12% is achieved using MY11 as p-type dopant to spiro-OMeTAD.

## Introduction

Dye-sensitized solar cells (DSCs), also known as the Grätzel cell, appear to be an alternative to silicon-based solar cells from an economic perspective.<sup>[1]</sup> Solid-state DSCs (ssDSCs) in which the volatile electrolyte was replaced by triarylamine-based hole-conductor such as 2,2',7,7'-tetrakis-(*N,N*-di-*p*-methoxyphenylamine)-9,9'-spirobifluorene (spiro-OMeTAD, Figure S1 in the Supporting Information),<sup>[2]</sup> CuSCN<sup>[3]</sup> and various conductive polymers [e.g., poly(3-hexylthiophen-2,5-diyl) (P3HT), polyaniline (PANI), and poly(3,4-ethylenedioxythiophene) (PEDOT)]<sup>[4–6]</sup> is expected to address the challenges associated with stability. Among all the hole-conductors, spiro-OMeTAD is still the choice for researchers in achieving high efficiency solid-state solar cells. However, the pristine form of spiro-OMeTAD possesses low conductivity, which directly affects photovoltaic parameters such as photocurrent and fill factor.<sup>[7,8]</sup> In order to overcome this limitation, doping to induce more charge carriers

within spiro-OMeTAD is essential for enhancing the device performance.

Initially, N(PhBr)<sub>3</sub>SbCl<sub>6</sub> was employed as a chemical dopant with an overall efficiency of 0.74% obtained.<sup>[2]</sup> Studies have also shown that spiro-OMeTAD can be oxidized in the presence of molecular oxygen under illumination.<sup>[9]</sup> However, the doping of spiro-OMeTAD through oxygen makes fabrication of the solar cell challenging and affects the reproducibility of the results. Therefore, chemical doping for spiro-OMeTAD becomes important.


High efficiency ssDSCs (7.2%) have been accomplished by using tris(2-(1*H*-pyrazol-1-yl)pyridine)cobalt(II) bis(hexafluorophosphate) (FK102) as p-dopant and Y123 as the organic sensitizer.<sup>[10]</sup> The energy difference between the highest occupied molecular orbital (HOMO) energy level of spiro-OMeTAD and redox potential of FK102 allows one-electron oxidation reaction to occur. The conductivity was enhanced by increasing the oxidized species of spiro-OMeTAD (spiro-OMeTAD<sup>+</sup>) upon doping with Co<sup>III</sup> p-dopant.

Chemical doping using Co dopant is beneficial for device fabrication in terms of reproducibility; however the device efficiency could still be limited by the unreacted dopant due to its non-ideal doping efficiency. In addition, the reacted dopant will also remain in the device. This implies that the reacted/unreacted Co complex will remain as defects in the device after depositing the hole-transporting layer. Thus, it is essential to reduce the amount of dopant used in doping, not only for reducing the overall cost but to also reduce the defects in the hole-transporting layer. In order to reduce the amount of dopant used, one should increase the driving force for the one-electron oxidation of spiro-OMeTAD to ensure higher spiro-to-spiro<sup>+</sup> conversion and decrease the amount of dopant necessary.

[a] T. M. Koh, S. Dharani, Dr. H. Li, R. R. Prabhakar, Prof. N. Mathews, Prof. S. G. Mhaisalkar  
Energy Research Institute @ NTU (ERI@N)  
Nanyang Technological University  
Research Techno Plaza  
Singapore 637553 (Singapore)  
E-mail: nripan@ntu.edu.sg

[b] T. M. Koh, S. Dharani, Prof. N. Mathews, Prof. A. C. Grimsdale, Prof. S. G. Mhaisalkar  
School of Materials Science & Engineering  
Nanyang Technological University  
Singapore 639798 (Singapore)  
E-mail: acgrimsdale@ntu.edu.sg

[c] Prof. N. Mathews  
Singapore-Berkeley Research Initiative for Sustainable Energy  
1 Create Way  
Singapore, 138602 (Singapore)

 Supporting Information for this article is available on the WWW under <http://dx.doi.org/10.1002/cssc.201400081>.

Recently, the emergence of organic inorganic halide perovskite-based solar cells has become a widely researched topic in photovoltaics.<sup>[11–13]</sup> Due to its narrow band gap<sup>[14]</sup> and long diffusion length,<sup>[15,16]</sup> perovskite-based photovoltaic devices have displayed high power conversion efficiencies approaching 15% under full sun illumination.<sup>[17–20]</sup> One of the possible ways to further increase its efficiency is to improve the photovoltage of the device by using alternative hole-conductors with a lower HOMO energy level. This would, in turn, also require the crucial development of Co dopants with a deep redox potential.

Herein, we designed a new p-dopant, tris[2-(1*H*-pyrazol-1-yl)pyrimidine]cobalt(III) tris[bis(trifluoromethylsulfonyl)imide] (MY11), in which the pyrazolyl moiety is coupled to a pyrimidine moiety instead of a pyridine moiety. Introduction of the pyrimidine core brings on a similar effect as incorporating electron-withdrawing group into the ligand which tunes the redox potential of the dopant more positively. By having a larger driving force for spiro one-electron oxidation reaction, we are able to reduce the amount of dopant used while still maintaining high efficiencies. High efficiency CH<sub>3</sub>NH<sub>3</sub>PbI<sub>3</sub> perovskite-based solar cells (Figure 1) were fabricated in order to eluci-

plexes.<sup>[21–23]</sup> By incorporating pyrazolyl moiety in molecular ligands, various cobalt complexes have been synthesized and used as redox couples<sup>[24]</sup> and dopants<sup>[10,25,26]</sup> in DSCs applications. Notable among these dopants is FK102 which has been proven to dope spiro-OMeTAD and was utilized in 7.2% ssDSCs along with highly absorbing organic dyes.<sup>[10]</sup> Figure 1b and 1c shows the chemical structures of FK102 and MY11.

In our newly designed Co dopant, MY11, we retain the pyrazolyl moiety in the ligand structure to keep the redox potential at a certain energy level to maintain the high driving force for spiro-OMeTAD one-electron oxidation reaction. Moreover, we replace the pyridine moiety (in FK102) by pyrimidine core in order to further lower the redox potential in MY11. Electron-withdrawing substituents such as chloride and nitro groups have been used to modulate the redox potential of metal complexes.<sup>[27]</sup> The presence of additional nitrogen atoms in the pyrimidine core in our designed ligand offers a similar electron-withdrawing effect as the cobalt center and tunes the redox potential of MY11 more than that of FK102. Instead of hexafluorophosphate (PF<sub>6</sub><sup>−</sup>) anion, bis(trifluoromethylsulfonyl)imide (TFSI<sup>−</sup>) anion was used for MY11 due to its better solubility<sup>[25]</sup> and, more importantly, higher electrochemical stability.<sup>[28]</sup>

Both FK102 and MY11 were obtained as orange solids and form pale orange solutions in organic solvents such as acetonitrile, methanol and dimethylformamide. The comparison of the optical absorption of these two dopants is depicted in Figure S2. The orange color solution arises from the weak d–d transition in the octahedral Co complexes at 400–600 nm. The low molar absorptivity (<200 L mol<sup>−1</sup> cm<sup>−1</sup>) of MY11 in the 400–600 nm region makes it an appropriate dopant for photovoltaic device.

Cyclic voltammograms of spiro-OMeTAD, FK102 and MY11 are shown in Figure 2a. CV results reveal that the first oxidation potential of spiro-OMeTAD is 0.62 V versus NHE whereas the redox potential of FK102 is 0.98 V versus NHE. The estimated driving force for spiro-OMeTAD one-electron oxidation reaction using FK102 is 360 mV which is in good agreement with the previous reported value.<sup>[10,25]</sup>

Compared to FK102, the redox potential of MY11 is further shifted to a more positive potential which is in agreement with our prediction, as mentioned earlier. The redox potential of MY11 was found to be 1.27 V versus NHE and the large shift of 290 mV in potential can be rationalized by the replacement of the three pyridine moieties with three pyrimidine cores in the ligands. It can be estimated that each pyrimidine core coordinated to the Co<sup>III</sup> metal center increases the redox potential by roughly 100 mV. Figure 2b shows the energy level diagram of the solar cell components and the red arrow indicates the increased driving force in MY11 compared to FK102 for spiro-OMeTAD oxidation reaction.

The oxidation of spiro-OMeTAD by Co dopants can be monitored through UV/Vis optical absorption spectroscopy. The optical absorption spectra of spiro-OMeTAD with additives and different dopants are illustrated in Figure 3. No absorption band for oxidized spiro-OMeTAD (spiro-OMeTAD<sup>+</sup>) was observed upon adding LiTFSI additives.<sup>[29]</sup> The absorption band of spiro-OMeTAD<sup>+</sup> at around 520 nm<sup>[30]</sup> was observed only when

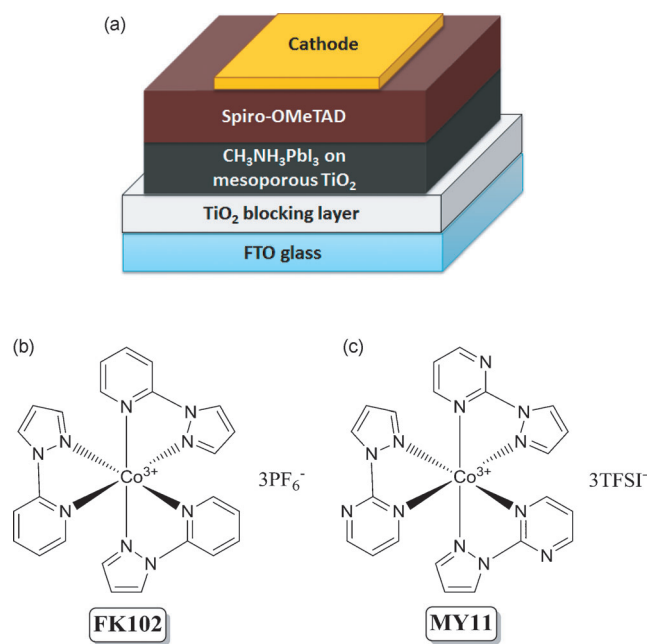


**Figure 1.** (a) Device structure of solar cell incorporating CH<sub>3</sub>NH<sub>3</sub>PbI<sub>3</sub> perovskite absorber. Chemical structures of (b) tris[2-(1*H*-pyrazol-1-yl)pyridine]cobalt(III) tris(hexafluorophosphate) (FK102) and (c) tris[2-(1*H*-pyrazol-1-yl)pyrimidine]cobalt(III) tris[bis(trifluoromethylsulfonyl)imide] (MY11).

date the effect of dopant on photovoltaic performance. An overall power conversion efficiency of 12% was accomplished by using this newly developed hole-transporting material (HTM) dopant.

## Results and Discussion

Studies have shown that pyrazole-containing ligands are weak donors and able to lower the redox potential of metal com-

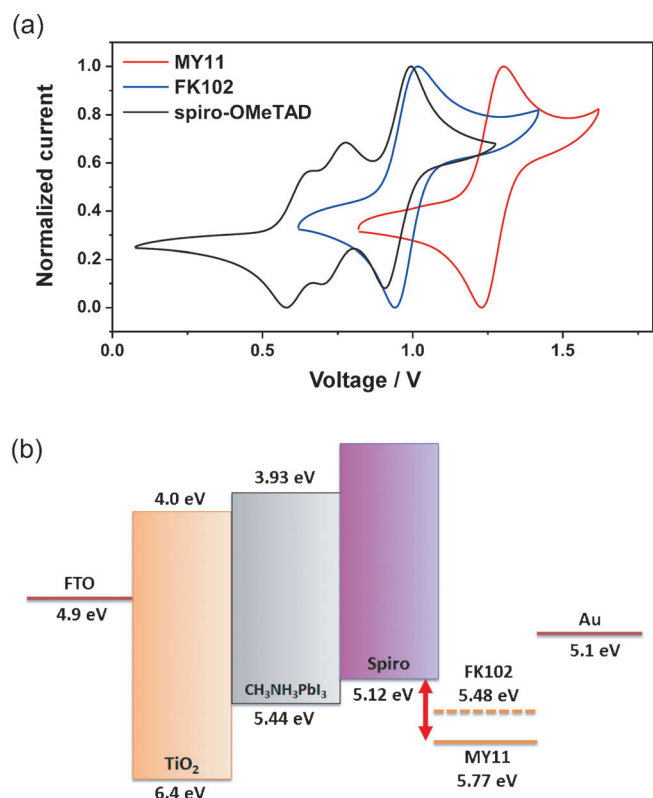


**Figure 2.** (a) Cyclic voltammograms of spiro-OMeTAD, FK102, and MY11. (b) Energy level diagram of  $\text{TiO}_2$ /perovskite/spiro-based solar cell with the redox potential of two Co dopants used in this study. The red arrow indicates the driving force for spiro-OMeTAD one-electron oxidation reaction.

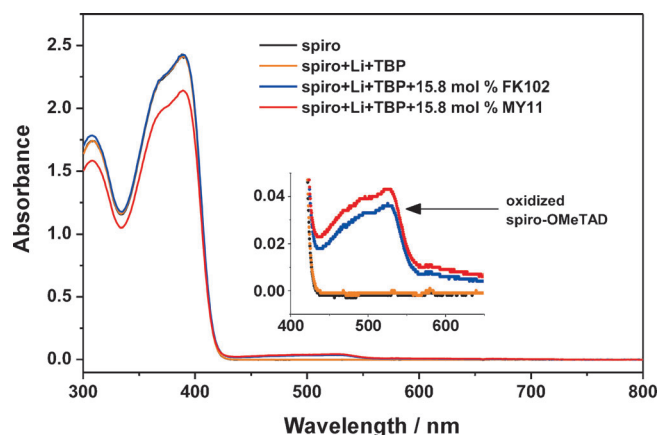


**Figure 3.** UV/Vis absorption spectra of spiro-OMeTAD with additives (LiTFSI and TBP) and dopants (FK102 or MY11). Inset shows the enlarged spectra of the oxidized spiro-OMeTAD peak at around 524 nm.

the Co dopant is added in our study. Due to the larger driving force for spiro-OMeTAD oxidation reaction in MY11, a higher spiro-to-spiro<sup>+</sup> conversion efficiency than FK102 is expected. The inset of Figure 3 shows the enlarged spectra between 400 to 600 nm and shows that the absorption of spiro-OMeTAD<sup>+</sup> is more intense in the solution with MY11 for the same doping concentration. This implies higher spiro-to-spiro<sup>+</sup> conversion efficiency in MY11 due to its larger potential difference be-

tween HOMO energy level of spiro-OMeTAD and its redox potential. The gradual addition of the MY 11 results in a gradual increased absorption of spiro-OMeTAD<sup>+</sup> as well in decreased absorption of the absorption band at approximately 390 nm. (see the Supporting Information Figure S3). The absorption band at 380–390 nm may involve the combination of the absorption of neutral spiro-OMeTAD, spiro-OMeTAD radical cation, and Co<sup>II</sup> complexes and their individual contributions are difficult to decouple.<sup>[25]</sup> Therefore, we only monitor the absorption band at around 520 nm which is purely contributed by spiro-OMeTAD oxidation.

It is known that pristine spiro-OMeTAD possesses low conductivity, which could be one of the limiting factors in achieving high efficiency solar cells. In order to understand the effect of doping using FK102 and MY11, we perform 4 probe conductivity measurements to investigate the change in conductivity of spiro-OMeTAD with and without dopant. The results are shown in Table 1. As expected, the pristine spiro-OMeTAD

**Table 1.** Comparison of conductivity of undoped spiro-OMeTAD and doped spiro-OMeTAD (with FK102 or MY11) films on glass substrates.

Sample	Conductivity [ $\text{S cm}^{-1}$ ]
pristine spiro	$5.21 \times 10^{-6}$
spiro + FK102	$1.35 \times 10^{-4}$
spiro + MY11	$1.69 \times 10^{-4}$

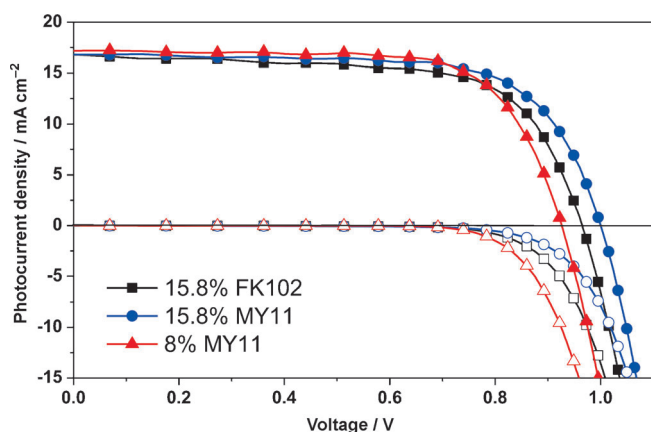
shows a low conductivity of  $5.21 \times 10^{-6} \text{ S cm}^{-1}$ , which is in agreement with the reported values.<sup>[10,29]</sup> Upon adding 15.8 mol% of FK102 and MY11 to spiro-OMeTAD (the same doping concentration as in device fabrication), the conductivities of the spiro films were found to be  $1.35 \times 10^{-4}$  and  $1.69 \times 10^{-4} \text{ S cm}^{-1}$ , respectively. Note that the conductivity of spiro-OMeTAD is enhanced by two orders of magnitude upon doping with MY11. The higher conductivity in MY11-containing spiro film can be explained by the higher spiro-to-spiro<sup>+</sup> conversion in MY11 due to its larger driving force for spiro-OMeTAD oxidation reaction, which has been clearly shown above. The conductivity results shown here are in agreement with our previous UV/Vis measurement that shows a greater amount of oxidized spiro-OMeTAD species are generated by doping with MY11 dopant. Owing to its higher spiro-to-spiro<sup>+</sup> conversion efficiency, reduced concentrations of MY11 can be used in device fabrication.

To elucidate the impact of our newly synthesized Co dopant, solar cells using  $\text{CH}_3\text{NH}_3\text{PbI}_3$  perovskite as absorber and spiro-OMeTAD as hole-conductor were fabricated. The photovoltaic performances of the device using FK102 and MY11 are summarized in Table 2 and corresponding  $I$ - $V$  curves are illustrated in Figure 4.

For the reference device (with FK102),  $J_{\text{sc}}$  of  $16.8 \text{ mA cm}^{-2}$ ,  $V_{\text{oc}}$  of 965 mV, FF of 0.68, and an overall efficiency of 11% was obtained. As described previously, the device with MY11 displays higher conductivity due to the increase in the amount of charge carrier, which has also been shown through UV/Vis measurement. Thus, a comparable photocurrent density is at-

**Table 2.** Photovoltaic parameters of perovskite-based devices shown in Figure 4.

Device	$J_{sc}$ [ $\text{mA cm}^{-2}$ ]	$V_{oc}$ [mV]	FF	$\eta$ [%]
15.8% FK102	16.8	965	0.68	11.0
15.8% MY11	16.8	1000	0.71	11.9
8.0% MY11	17.2	927	0.71	11.4

**Figure 4.** Photocurrent-voltage ( $J$ - $V$ ) characteristics (light intensity:  $100 \text{ mW cm}^{-2}$ , AM1.5G). Every 5th data point is marked with a symbol.

tained in the device with 15.8% MY11; the better power conversion efficiency in the MY11-containing devices is mainly attributed to its improved photovoltage as well as to the fill factor of the devices. Generally, photovoltage of a device is determined by the difference between Fermi energy level of  $\text{TiO}_2$  and HOMO energy level of spiro-OMeTAD.<sup>[2]</sup> The open-circuit voltage is improved from 965 mV in the device containing 15.8% FK102 to 1000 mV in the device containing 15.8% MY11, which is most probably due to the increased concentration of oxidized spiro-OMeTAD. An earlier report has shown that the increased hole concentration could induce the shift of Fermi level toward the HOMO level in spiro-OMeTAD conductors, resulting in enhanced  $V_{oc}$ .<sup>[31]</sup> The higher FF (0.71) in the device containing 15.8% MY11 are probably due to the additional charge carriers that are generated by MY11, which in turn increase the conductivity of the film and reduce the series resistance in the solar cell.

Since the MY11 possesses larger driving force for the spiro-OMeTAD one-electron oxidation reaction, the doping concentration in the device can be reduced. When the doping concentration is reduced to 8 mol%, the  $V_{oc}$  of the device is decreased to 927 mV. It can be rationalized that there are fewer spiro-OMeTAD<sup>+</sup> species in the device and the Fermi level remains further away from the HOMO energy level of spiro-OMeTAD, which in turn results in the loss of photovoltage. However, the FF is still maintained as high as in the 15.8% MY11 device and a slightly higher photocurrent density is obtained, yielding an overall efficiency of 11.4%. The incident photo-to-current efficiency (IPCE) plots of the devices in Figure S4 shows no significant change in the absorption of perovskite when MY11 is used for the replacement of FK102. Thus,

MY11 does not affect the light harvesting of the device and exhibits promising dopant properties in solar cell application.

## Conclusions

We synthesized a new cobalt complex, MY11, with a deep redox potential as dopant for organic hole-conductors. We demonstrated the tuning of redox potential of the Co dopant by incorporating a pyrimidine moiety in the ligand. Through the optical and electrochemical analysis, the newly synthesized dopant shows effective spiro-to-spiro<sup>+</sup> conversion and excellent dopant properties in photovoltaic applications. An overall power conversion efficiency of 12% has been accomplished using MY11 as p-type dopant. To the best of our knowledge, MY11 possesses the deepest redox potential among all the current cobalt-based dopant and allows it to be a potent dopant for a wide range of hole-transport materials in photovoltaic applications.

## Experimental Section

### Synthesis of tris[2-(1*H*-pyrazol-1-yl)pyridine]cobalt(II) bis(hexafluorophosphate)

Briefly, to a methanolic solution containing 1 equivalent  $\text{CoCl}_2 \cdot 6\text{H}_2\text{O}$  (Sigma Aldrich), 3.1 equivalents of tris[2-(1*H*-pyrazol-1-yl)pyridine]<sup>[10]</sup> ligand was added. The solution was heated with stirring at 60 °C for 2 h. The solution was cooled to room temperature and a tenfold excess of ammonium hexafluorophosphate ( $\text{NH}_4\text{PF}_6$ , Sigma Aldrich) aqueous solution was added into the solution. The solution was stirred for another 30 min at room temperature and kept in the refrigerator overnight for complete precipitation. The orange solid was filtered and washed with water. The desired complex was obtained upon drying under vacuum. Yield: 94%.

### Synthesis of tris[2-(1*H*-pyrazol-1-yl)pyridine]cobalt(III) tris(hexafluorophosphate) (FK102)

1 equivalent of tris[2-(1*H*-pyrazol-1-yl)pyridine]cobalt(II) bis(hexafluorophosphate) was dissolved in a minimal amount of acetonitrile and an excess (2 equivalents) of  $\text{NOBF}_4$  (Sigma Aldrich) was added to the solution. The solution was stirred for 30 min at room temperature. A fivefold excess of  $\text{NH}_4\text{PF}_6$  aqueous solution was added and stirred for another 30 min. The orange solid formed was collected by filtration and washed with water. FK102 was obtained upon drying under vacuum. Yield: 92%.

### Synthesis of 2-(1*H*-pyrazol-1-yl)pyrimidine

1 equivalent of pyrazole (Sigma Aldrich) and 1.2 equivalent of potassium *tert*-butoxide (Sigma Aldrich) were dissolved in dimethyl sulfoxide and stirred at room temperature until complete dissolution. 0.9 equivalent of 2-chloropyrimidine (Sigma Aldrich) was added into the solution and heated for 4 h at 100 °C. The solution was cooled down to room temperature and extracted three times with water/dichloromethane. The organic phases were combined and dried using rotary evaporator. The desired compound was obtained as oil. Yield: 82%. <sup>1</sup>H NMR (400 MHz,  $\text{CDCl}_3$ ):  $\delta$  = 8.69 (d, 2H, ArH), 8.54 (d, 1H, ArH), 7.78 (d, 1H, ArH), 7.15 (t, 1H, ArH),



6.45 ppm (d, 1H, ArH).  $^{13}\text{C}$  NMR (400 MHz,  $\text{CDCl}_3$ ):  $\delta$  = 159.5, 156.6, 144.3, 129.8, 119.3, 109.4 ppm.

### Synthesis of tris[2-(1H-pyrazol-1-yl)pyrimidine]cobalt(II) bis[bis(trifluoromethylsulfonyl)imide]

The cobalt complex was synthesized using the same procedure as described above for tris[2-(1H-pyrazol-1-yl)pyridine]cobalt(II) bis(hexafluorophosphate) by replacing the ligand and salt with 2-(1H-pyrazol-1-yl)pyrimidine and lithium bis(trifluoromethylsulfonyl)imide respectively. Yield: 94%.

### Synthesis of tris[2-(1H-pyrazol-1-yl)pyrimidine]cobalt(III) tris[bis(trifluoromethylsulfonyl)imide] (MY11)

MY11 was synthesized using the same procedure as described above for FK102 by replacing the ligand and salt with 2-(1H-pyrazol-1-yl)pyrimidine and lithium bis(trifluoromethylsulfonyl)imide respectively. Yield: 80%.  $^1\text{H}$  NMR (400 MHz,  $\text{CD}_3\text{CN}$ ):  $\delta$  = 9.25 (m, 3H, ArH), 9.10 (m, 3H, ArH), 7.91–7.79 (m, 6H, ArH), 7.67–7.59 (m, 3H, ArH), 7.13 ppm (m, 3H, ArH).

### Solar cell fabrication

Fluorine doped tin oxide (FTO) substrate was etched using Zn powder and 4 M hydrochloric acid (HCl) and subsequently cleaned with Decon soap solution and ethanol. The substrate was then immersed in 40 mM of  $\text{TiCl}_4$  solution for 30 min at 70 °C. A thin compact layer of  $\text{TiO}_2$  (blocking layer) was deposited by aerosol spray-pyrolysis at 450 °C. For spray pyrolysis, a solution of titanium diisopropoxide bis(acetylacetonate) (75 wt% in isopropanol) and absolute ethanol (ratio 1:9 by volume) was used. Nanocrystalline  $\text{TiO}_2$  film was deposited by spin-coating  $\text{TiO}_2$  paste on the substrate and it was calcined at 500 °C for 30 min. Then the substrate was again immersed in 40 mM of  $\text{TiCl}_4$  solution for 30 min at 70 °C, followed by sintering at 500 °C for 30 min.

The  $\text{CH}_3\text{NH}_3\text{PbI}_3$  perovskite layer was deposited by sequential method as reported in literature.<sup>[19]</sup> Lead iodide solution (1 M in dimethylformamide) was spin-coated on the substrate at 6000 rpm for 5 s. The substrate was then dried for 30 min at 70 °C. The film was subsequently dipped in  $\text{CH}_3\text{NH}_3\text{I}$  solution (10 mg mL<sup>-1</sup> in 2-propanol) for approx. 20 min. Then the film was rinsed with 2-propanol and dried at 70 °C for 30 min.

Spiro-OMeTAD solution (120 mg mL<sup>-1</sup> in chlorobenzene) was spin-coated on the perovskite spin-coated substrate. Lithium bis(trifluoromethylsulfonyl)imide, *tert*-butylpyridine and cobalt dopant were added to the above solution.<sup>[19]</sup> Gold counter electrode was deposited using thermal evaporation method.

### Characterization techniques

For the photovoltaic measurements, all devices (0.2 cm<sup>2</sup> active area) were measured by using San-EI Electric, XEC-301S solar simulator (San-EI Electric, XEC-301S) under AM 1.5G standard with a 0.25 cm<sup>2</sup> black mask. *J*–*V* characteristics were recorded using with a Keithley (model 2612A) digital source meter. Incident photon to current efficiency (IPCE) was performed using PVE300 (Bentham), with dual Xenon/quartz halogen light source, measured in DC mode with no bias light used. Cyclic voltammetry was carried out using a three-electrode setup with 0.1 Vs<sup>-1</sup> where platinum was used as working electrode, glassy carbon as counter electrode, and aqueous Ag/AgCl as reference electrode. UV/Vis mea-

surement was performed using Shimadzu UV-3600 UV/Vis–NIR spectrophotometer. Resistivity of the HTM films was measured in a four-probe configuration (MMR technologies). Four square electrodes (1.6 mm × 1.6 mm) of gold were thermally evaporated in square geometry onto the spiro-OMeTAD films which were spin-coated on glass substrate.

### Acknowledgements

Funding from National Research Foundation (NRF), Singapore, is acknowledged through CRP Award No.: NRF-CRP4-2008-03 and the Singapore-Berkeley Research Initiative for Sustainable Energy (SinBeRISE) CREATE programme.

**Keywords:** cobalt complex • electrochemistry • dye-sensitized solar cells • perovskites • redox potential

- [1] B. O'Regan, M. Grätzel, *Nature* **1991**, 353, 737–740.
- [2] U. Bach, D. Lupo, P. Comte, J. E. Moser, F. Weissortel, J. Salbeck, H. Spreitzer, M. Grätzel, *Nature* **1998**, 395, 583–585.
- [3] Y. Itzhak, O. Niitsoo, M. Page, G. Hodes, *J. Phys. Chem. C* **2009**, 113, 4254–4256.
- [4] J. B. Xia, N. Masaki, M. Lira-Cantu, Y. Kim, K. J. Jiang, S. Yanagida, *J. Am. Chem. Soc.* **2008**, 130, 1258–1263.
- [5] W. Zhang, R. Zhu, F. Li, Q. Wang, B. Liu, *J. Phys. Chem. C* **2011**, 115, 7038–7043.
- [6] W. Zhang, Y. M. Cheng, X. O. Yin, B. Liu, *Macromol. Chem. Phys.* **2011**, 212, 15–23.
- [7] F. Fabregat-Santiago, J. Bisquert, E. Palomares, S. A. Haque, J. R. Durrant, *J. Appl. Phys.* **2006**, 100, 034510.
- [8] F. Fabregat-Santiago, J. Bisquert, L. Cevey, P. Chen, M. K. Wang, S. M. Za-keeruddin, M. Grätzel, *J. Am. Chem. Soc.* **2009**, 131, 558–562.
- [9] U. B. Cappel, T. Daeneke, U. Bach, *Nano Lett.* **2012**, 12, 4925–4931.
- [10] J. Burschka, A. Dualeh, F. Kessler, E. Baranoff, N. L. Cevey-Ha, C. Y. Yi, M. K. Nazeeruddin, M. Grätzel, *J. Am. Chem. Soc.* **2011**, 133, 18042–18045.
- [11] A. Kojima, K. Teshima, Y. Shirai, T. Miyasaka, *J. Am. Chem. Soc.* **2009**, 131, 6050–6051.
- [12] N. G. Park, *J. Phys. Chem. Lett.* **2013**, 4, 2423–2429.
- [13] H. J. Snaith, *J. Phys. Chem. Lett.* **2013**, 4, 3623–3630.
- [14] J. H. Im, C. R. Lee, J. W. Lee, S. W. Park, N. G. Park, *Nanoscale* **2011**, 3, 4088–4093.
- [15] G. C. Xing, N. Mathews, S. Y. Sun, S. S. Lim, Y. M. Lam, M. Grätzel, S. Mhaisalkar, T. C. Sum, *Science* **2013**, 342, 344–347.
- [16] S. D. Stranks, G. E. Eperon, G. Grancini, C. Menelaou, M. J. P. Alcocer, T. Leijtens, L. M. Herz, a. Petrozza, H. J. Snaith, *Science* **2013**, 342, 341–344.
- [17] H. S. Kim, C. R. Lee, J. H. Im, K. B. Lee, T. Moehl, A. Marchioro, S. J. Moon, R. Humphry-Baker, J. H. Yum, J. E. Moser, M. Grätzel, N. G. Park, *Sci. Rep.* **2012**, 2, 591.
- [18] M. M. Lee, J. Teuscher, T. Miyasaka, T. N. Murakami, H. J. Snaith, *Science* **2012**, 338, 643–647.
- [19] J. Burschka, N. Pellet, S. J. Moon, R. Humphry-Baker, P. Gao, M. K. Nazeeruddin, M. Grätzel, *Nature* **2013**, 499, 316–319.
- [20] J. H. Heo, S. H. Im, J. H. Noh, T. N. Mandal, C. S. Lim, J. A. Chang, Y. H. Lee, H. J. Kim, A. Sarkar, M. K. Nazeeruddin, M. Grätzel, S. I. Seok, *Nat. Photonics* **2013**, 7, 486–492.
- [21] D. L. Jameson, J. K. Blaho, K. T. Kruger, K. A. Goldsby, *Inorg. Chem.* **1989**, 28, 4312–4314.
- [22] T. Ayers, S. Scott, J. Goins, N. Caylor, D. Hathcock, S. J. Slattey, D. L. Jameson, *Inorg. Chim. Acta* **2000**, 307, 7–12.
- [23] M. A. Halcrow, *Coord. Chem. Rev.* **2005**, 249, 2880–2908.
- [24] S. Ahmad, T. Bessho, F. Kessler, E. Baranoff, J. Frey, C. Y. Yi, M. Grätzel, M. K. Nazeeruddin, *Phys. Chem. Chem. Phys.* **2012**, 14, 10631–10639.
- [25] J. Burschka, F. Kessler, M. K. Nazeeruddin, M. Grätzel, *Chem. Mater.* **2013**, 25, 2986–2990.

- [26] J. H. Noh, N. J. Jeon, Y. C. Choi, M. K. Nazeeruddin, M. Grätzel, S. I. Seok, *J. Mater. Chem. A* **2013**, *1*, 11842–11847.
- [27] S. M. Feldt, G. Wang, G. Boschloo, A. Hagfeldt, *J. Phys. Chem. C* **2011**, *115*, 21500–21507.
- [28] H. Djellab, M. Armand, D. Delabouglise, *Synth. Met.* **1995**, *74*, 223–226.
- [29] H. J. Snaith, M. Grätzel, *Appl. Phys. Lett.* **2006**, *89*, 262114.
- [30] S. Fantacci, F. De Angelis, M. K. Nazeeruddin, M. Grätzel, *J. Phys. Chem. C* **2011**, *115*, 23126–23133.
- [31] R. Schölin, M. H. Karlsson, S. K. Eriksson, H. Siegbahn, E. M. J. Johansson, H. Rensmo, *J. Phys. Chem. C* **2012**, *116*, 26300–26305.

---

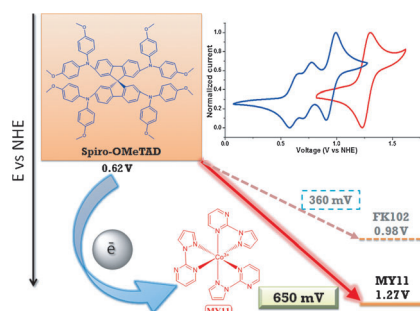
Received: January 21, 2014

Revised: March 12, 2014

Published online on ■ ■ ■■, 0000

## FULL PAPERS

**Superiority complex:** A new cobalt complex with deep redox potential is synthesized as p-dopant for hole-transporting materials in photovoltaic devices. High efficiency perovskite-based solar cells are fabricated using the complex as dopant for molecular hole-conductor 2,2',7,7'-tetrakis-(*N,N*-di-*p*-methoxyphenylamine)-9,9'-spirobifluorene. The dopant shows effective spiro-to-spiro<sup>+</sup> conversion and excellent dopant properties in photovoltaic applications.



*T. M. Koh, S. Dharani, H. Li,  
R. R. Prabhakar, N. Mathews,\*  
A. C. Grimsdale,\* S. G. Mhaisalkar*



**Cobalt Dopant with Deep Redox Potential for Organometal Halide Hybrid Solar Cells**

